

Quantum speed limits on operator flows and correlation functions

Nicoletta Carabba,¹ Niklas Hörnfeldt,^{1,2} and Adolfo del Campo^{1,3}

¹*Department of Physics and Materials Science, University of Luxembourg, L-1511 Luxembourg, G. D. Luxembourg*

²*Fysikum, Stockholms Universitet, 106 91 Stockholm, Sweden*

³*Donostia International Physics Center, E-20018 San Sebastián, Spain*

(Dated: September 13, 2022)

Quantum speed limits (QSLs) identify fundamental time scales of physical processes by providing lower bounds on the rate of change of a quantum state or the expectation value of an observable. We introduce a generalization of QSL for unitary operator flows, which are ubiquitous in physics and relevant for applications in both the quantum and classical domains. We derive two types of QSLs and assess the existence of a crossover between them, that we illustrate with a qubit and a random matrix Hamiltonian, as canonical examples. We further apply our results to the time evolution of autocorrelation functions, obtaining computable constraints on the linear dynamical response of quantum systems out of equilibrium and the quantum Fisher information governing the precision in quantum parameter estimation.

I. INTRODUCTION

Unraveling the fundamental time scale of a physical process is crucial in many theoretical and experimental scenarios. Quantum speed limits (QSLs) constitute a set of fundamental results in quantum physics that bound the minimum time for a physical process to happen. Although their initial formulation [1, 2] was restricted to unitary evolution between two pure quantum states, by now they have been generalized to the case of arbitrary mixed states [3, 4], driven Hamiltonians [3, 5–7], open quantum dynamics [8–11], continuous quantum measurements [12], and classical processes [13–15]. Their applications are thus manifold and range over various branches of physics [16]. Their use is prominent in quantum technologies, including quantum computation [17, 18] and quantum metrology [19, 20]. QSLs are known to limit the performance of quantum control algorithms [21, 22], and play a key role in shortcuts to adiabaticity by counter-diabatic driving both in isolated [23, 24] and open quantum systems [25, 26]. They have also been applied to many-body physics, in which care is needed given the orthogonality catastrophe [27–31]. In addition, some formulations of QSLs have transcended the notion of quantum state distinguishability and focused on the rate of change of other quantities such as quantum coherence [32–34], and more generally, quantum resources [35].

Bounds to the pace of evolution naturally have important implications in nonequilibrium thermodynamics. In this context, the connection between QSLs and thermodynamic uncertainty relations (TURs) [36, 37] has been explored in [38, 39], identifying QSL-inspired constraints on non-equilibrium fluctuations. Recently, a closely related work [40], following the initial spirit of [1], established a generalized QSL on the evolution of observables, in particular, of their expectation values, under arbitrary dynamics. The notion of the speed of an observable expectation value was also considered in [30, 31, 41].

A natural question then arises: is it possible to formulate QSLs directly on the operator flow, rather than on

the time-dependent expectation value of an observable? An operator flow describes the evolution of an operator under some given dynamics. In the unitary case, the evolution of the operator results from its conjugation by a unitary. Unitary operator flows are ubiquitous in physics, ranging from the quantum evolution of an observable in the Heisenberg picture to the Lax pair flow in classical integrable systems and continuous renormalization group flows, such as the one proposed by Wegner [42]. Preceding efforts in this direction have focused on the preparation of unitary [43] and non-unitary [44] quantum operations in the context of quantum control. Moreover, a Liouville space formulation of the QSL on the evolution of density matrices was introduced in [45]. However, a framework to describe general operator flows, for general operators, is still lacking. Constraining the speed of these flows would naturally prove useful also in characterizing operator growth [46–50], which has attracted increasing attention as a powerful approach to describe the buildup of complexity in quantum systems, in parallel to the earlier notion of quantum state complexity [51], that is also subject to QSLs [52–55]. In this context, a QSL-like uncertainty bound has recently been introduced [56] on the growth of a particular notion of operator complexity, known as Krylov complexity [57–60].

In this manuscript, we introduce two notions of QSL for operator flows. Although we focus on the unitary time evolution in the Heisenberg picture, our results can be applied to a wider class of unitary flows, including some examples of inhomogeneous flows. Moreover, they do not require the flowing operator to be Hermitian. In addition, we introduce QSLs for the two-point autocorrelation functions, which play a key role in many-body physics, determine the linear response [61] and transport properties of a quantum system, and characterize the operator growth in Krylov space. The exact computation of correlation functions is generally a challenging task, requiring solving the dynamics, while our bounds are easy to compute provided that the Hamiltonian and the initial operator are known. Our results show the presence of a universal crossover between an initial regime in which the

dynamics follows a Mandelstam-Tamm (MT) [1] type of QSL and a second one in which a Margolus-Levitin (ML) [2] type of QSL yields a more accurate description. We illustrate this crossover, analogous to that recently observed experimentally for quantum state evolution [62], in the case of a two-level system and of a random matrix Hamiltonian. Furthermore, our results provide easily computable constraints on the non-equilibrium dynamical response of arbitrary systems to an external perturbation within linear response theory. Finally, exploiting the relation between the dynamical susceptibility and the quantum Fisher information [63], we upper bound this quantity with an easily computable correlation function.

II. QUANTUM SPEED LIMITS FOR OPERATORS

The paradigmatic example of operator flow in quantum mechanics is the unitary flow $\dot{O}_t = \frac{i}{\hbar}[H, O_t]$, describing the time evolution of an initial operator O_0 generated by the Liouvillian $\mathbb{L}[\cdot] = \frac{i}{\hbar}[H, \cdot]$. The unitary character of the flow is manifest in the formal solution $O_t = U_t^\dagger O_0 U_t$, where $U_t = \exp(-itH/\hbar)$ is the unitary time-evolution operator associated with a time-independent Hamiltonian H . It is convenient to visualize this flow upon vectorizing operators in Liouville space, as it allows a direct analogy between operator flow and quantum state evolution. Therefore, let us represent a general bounded operator $A = \sum_{i,j} A_{ij} |i\rangle\langle j|$, where $\{|i\rangle\}$ can be any basis of the Hilbert space, as a normalized vector

$$|A\rangle = \frac{1}{\|A\|} \sum_{i,j} A_{ij} |i\rangle\langle j|, \quad (1)$$

where $\|A\| = \sqrt{\langle A, A \rangle}$ is the Hilbert-Schmidt norm associated with the Hilbert-Schmidt inner product $\langle A, B \rangle = \text{Tr}[A^\dagger B]$. In Liouville space, the latter is proportional to the standard scalar product over \mathbb{C}^{d^2} , being $\langle A, B \rangle = \|A\| \|B\| \langle A|B \rangle$. In the isomorphic real vector space \mathbb{R}^{2d^2} the real part $\text{Re} \langle A, B \rangle$ defines the standard Euclidean inner product.

Let us now consider the Heisenberg evolution of an operator O_0 generated by a time-independent Hamiltonian H . For the moment, we do not restrict ourselves to observables, meaning that O_0 can also be non-Hermitian. In Liouville space, we can rewrite the Heisenberg equation as $\partial_t |O_t\rangle = \mathbb{L} |O_t\rangle$, where the Liouvillian, which, with a slight abuse of notation, we shall continue to indicate as \mathbb{L} , takes the form

$$\mathbb{L} = \frac{i}{\hbar}(H \otimes \mathbb{1} - \mathbb{1} \otimes H^T). \quad (2)$$

A particularly useful object to quantify the displacement of the operator along the flow is the operator overlap

$$\langle O_0 | O_t \rangle = \frac{\text{Tr}(O_0^\dagger O_t)}{\|O\|^2}, \quad (3)$$

which can be complex in general and becomes real when Hermitian operators are considered. A key observation is that the operator overlap is proportional to the infinite temperature autocorrelation function: we shall see how this feature will allow us to extend our result to finite-temperature autocorrelation functions as well. Note that $\langle O_0 | O_t \rangle$ is closely related to the notion of operator fidelity introduced in the context of Loschmidt echoes and quantum phase transitions [64].

To measure how “far” the operator O_t has flowed, we define the operator angle \mathcal{L}_t between the vector $|O_t\rangle$ and the initial one $|O_0\rangle$:

$$\mathcal{L}_t \equiv \arccos \text{Re} \langle O_0 | O_t \rangle. \quad (4)$$

This quantity defines a distance over the unitary flow $O_t = U_t^\dagger O_0 U_t$. Being the vectorized operator normalized as in Eq. (1), the unitary flow in Liouville space lies on the unit sphere. Since $\text{Re} \langle O_0 | O_t \rangle$ is the Euclidean inner product, Eq. (4) reduces to the angle between the corresponding real vectors in \mathbb{R}^{2d^2} and is therefore a distance. We also note that \mathcal{L}_t resembles the notion of Bures angle $\ell = \arccos |\langle \psi_0 | \psi_t \rangle|$, but it does not reduce to it when the initial operator is chosen to be the projector over the pure state $|\psi_0\rangle$, $O_0 = |\psi_0\rangle\langle\psi_0|$. Moreover, let us stress that $\arccos |\langle O_0 | O_t \rangle|$ would not be a good notion of distance between operators, as it would vanish every time they differ only by a phase. While physical states are defined up to an irrelevant global phase, the same is not true for operators, as global phases between observable are physical. Said differently, the fact that Liouville space is a Hilbert space but not a projective Hilbert space favors the use of the distance (4) over the conventional Bures angle.

Now, let $\{|i\rangle\}$ be the energy eigenbasis, such that $H|i\rangle = E_i |i\rangle$, and let the initial operator be $O_0 = \sum_{ij} O_{ij} |i\rangle\langle j|$ in such basis. The Liouvillian is diagonal in the vectorized basis $|i\rangle\otimes|j\rangle$ and has the energy gaps $\Delta_{ij} \equiv E_i - E_j$ as diagonal entries. The operator overlap takes the form

$$\langle O_0 | O_t \rangle = \frac{1}{\|O\|^2} \sum_{j,k} e^{i\Delta_{jk}t/\hbar} |O_{jk}|^2. \quad (5)$$

Using trigonometric inequalities, we can derive two QSLs in terms of the operator overlap, which, as we will argue below, can be regarded as the generalization of the Margolus-Levitin (ML) [2] and Mandelstam-Tamm (MT) [1] QSLs for Schrödinger evolution. Indeed, by using that $\cos x \geq 1 - \alpha|x|$, where the parameter $\alpha \approx 0.724$ is chosen such that $1 - \alpha x$ is tangent to $\cos x$ for $x > 0$ [65], we can bound the real part of the overlap from below,

$$\text{Re} \langle O_0 | O_t \rangle \geq 1 - \frac{\alpha t}{\hbar \|O\|^2} \sum_{j,k} |\Delta_{jk}| |O_{jk}|^2 = 1 - \alpha \langle |\mathbb{L}| \rangle t, \quad (6)$$

where the brackets in the right-hand side stand for the expectation value over the vectorized operator: $\langle \cdot \rangle = \langle O_0 | \cdot | O_0 \rangle$. Further, its time derivative $\text{Re} \langle O_0 | \dot{O}_t \rangle$ can

be upper bounded by making use of the inequality $-x^2 \leq x \sin x \leq x^2$, valid $\forall x$:

$$|\operatorname{Re} \langle O_0 | \dot{O}_t \rangle| \leq \frac{t}{\hbar^2 \|O\|^2} \sum_{j,k} \Delta_{jk}^2 |O_{jk}|^2 = \langle \mathbb{L}^2 \rangle t. \quad (7)$$

The derivative of the operator overlap is related to that of the operator angle \mathcal{L}_t by

$$\operatorname{Re} \langle O_0 | \dot{O}_t \rangle = -\sin(\mathcal{L}_t) \dot{\mathcal{L}}_t, \quad (8)$$

which, after time integration, when combined with Eq. (7), yields

$$1 - \cos \mathcal{L}_t \leq \frac{\langle \mathbb{L}^2 \rangle}{2} t^2. \quad (9)$$

Therefore, from Eqs. (6) and (9) we obtain the two following QSLs, formulated in terms either of the operator overlap or the operator angle:

$$t \geq \frac{1 - \operatorname{Re} \langle O_0 | O_t \rangle}{\alpha \langle |\mathbb{L}| \rangle} = \frac{1 - \cos \mathcal{L}_t}{\alpha \langle |\mathbb{L}| \rangle}, \quad (10)$$

$$t \geq \sqrt{\frac{2(1 - \operatorname{Re} \langle O_0 | O_t \rangle)}{\langle \mathbb{L}^2 \rangle}} = \sqrt{\frac{2(1 - \cos \mathcal{L}_t)}{\langle \mathbb{L}^2 \rangle}}. \quad (11)$$

These results identify $\langle |\mathbb{L}| \rangle$ and $\sqrt{\langle \mathbb{L}^2 \rangle}$ as upper bounds on the speeds of the operator flow. We stress that the quantities $\langle |\mathbb{L}| \rangle$ and $\langle \mathbb{L}^2 \rangle$ are time independent under unitary dynamics, when the evolution is generated by a time-independent Hamiltonian. Moreover, we note that if O_0 is Hermitian the operator overlap is real at any time and $\langle \mathbb{L} \rangle = 0$ by parity, so that $\langle \mathbb{L}^2 \rangle = (\Delta \mathbb{L})^2$ is the variance of the Liouvillian. The analogy with ML and MT bounds, at least for flows of observables, is already evident. Both for state and operator evolution, the relevant time scale is given in terms of the mean and the variance of the generator of evolution, for ML and MT bounds, respectively. In the case of states, the generator is the Hamiltonian H , while in Liouville space the dynamics of operator flows is generated by the Liouvillian \mathbb{L} . We observe that, in the case of operator evolution, the ML bound (10) is given in terms of $\langle |\mathbb{L}| \rangle$ rather than the mean of the generator $\langle \mathbb{L} \rangle$, as this one vanishes for Hermitian operators. Let us further note that, by using other trigonometric inequalities, one can derive analogous QSLs that are proportional to Eqs. (10)-(11) through a numerical constant smaller than one, thus yielding a weaker result, see App. A.

It is instructive to identify which operators maximize the upper bounds $\langle |\mathbb{L}| \rangle$ and $\sqrt{\langle \mathbb{L}^2 \rangle}$ on the speed of the flow for a given Hamiltonian, as these will undergo the fastest operator growth. By looking at Eqs. (7) and (6), and noting that $(|O_{ij}|/\|O\|)^2 \leq 1$ defines a proper probability distribution over the energy states pairs, it is clear that the operators O_{\max} flowing at the maximal speed are the ones whose non-zero elements are only between energy eigenstates with the maximum gap $|\Delta_{\max}| = E_{\max} - E_0$, where E_{\max} and E_0 are the

highest and the lowest energy eigenvalues, respectively. This maximal speed is the analogous for operators of the one identified by the dual ML bound, recently introduced for state evolution [66]. If these levels are non-degenerate, the fastest operator will be of the form $O_{\max} = \mu |E_{\max}\rangle \langle E_0| + \nu |E_0\rangle \langle E_{\max}|$ for some complex constant μ and ν ($\mu = \nu^*$ for observables). This is analogous to the well-known result for states [67].

Remarkably, the above QSLs identify a universal crossover between two different time regimes. At early times $t \leq \tau_c$, being $\tau_c = 2\alpha \langle |\mathbb{L}| \rangle / \langle \mathbb{L}^2 \rangle$ the crossover time, the decay of the operator overlap is governed by a quadratic MT bound

$$\operatorname{Re} \langle O_0 | O_t \rangle \geq 1 - \frac{\langle \mathbb{L}^2 \rangle}{2} t^2, \quad (12)$$

while for times $t \geq \tau_c$ the linear ML bound

$$\operatorname{Re} \langle O_0 | O_t \rangle \geq 1 - \alpha \langle |\mathbb{L}| \rangle t \quad (13)$$

becomes tighter. A similar crossover was experimentally observed for the state fidelity of a single atom in an optical trap [62].

Furthermore, let us note that the QSLs (10) and (11) can be recast in terms of the Hamiltonian H , which generates the time evolution in the Hilbert space, rather than the Liouvillian, i.e., the generator of evolution in Liouville space. This reformulation will prove advantageous in expressing the relevant timescales as thermal expectation values. Indeed, $\sqrt{\langle \mathbb{L}^2 \rangle}$ is proportional to the norm of the operator velocity

$$\sqrt{\langle \mathbb{L}^2 \rangle} = \frac{1}{\hbar} \frac{\| [H, O_t] \|}{\| O \|} = \frac{\| \partial_t O \|}{\| O \|}, \quad (14)$$

which, as emphasized, is time-independent under unitary dynamics. Regarding the ML QSL, by using that $|\Delta_{jk}| \leq E_j + E_k - 2E_0$ in terms of the ground state energy E_0 , we find

$$\langle |\mathbb{L}| \rangle \leq \frac{1}{\hbar} \frac{\operatorname{Tr}(O_0^\dagger \{H - E_0, O_0\})}{\| O \|^2}. \quad (15)$$

Therefore, the ML QSL can be recast as

$$t \geq \hbar \frac{\| O \|^2}{\alpha} \frac{1 - \operatorname{Re} \langle O_0 | O_t \rangle}{\operatorname{Tr}(O_0^\dagger \{H - E_0, O_0\})}, \quad (16)$$

which is generally weaker than the original Liouvillian bound (10). We shall make use of these results in the next section, to bound the rate of change of autocorrelation functions.

Finally, if we choose $O_0 = |\psi_0\rangle \langle \psi_0|$ and let it evolve backward in time, thus recovering the corresponding forward time evolution of the state $|\psi_0\rangle$ in the Schrödinger picture, we find that the bounds (10) and (11) become proportional to the standard ML and MT QSLs in the case of orthogonal state evolution, thus justifying the given interpretation, see App. B. We note that the proportionality constant is smaller than one, meaning that

our bounds are not violated. However, they cannot be tight for state evolution. Furthermore, the result (B12) can be extended to driven dynamics, under the assumption that the energy eigenvectors are stationary, see App. C.

The general results derived in this section can be applied in a variety of theoretical settings. In particular, as shown below, the QSLs on operator flows bound the decay of autocorrelation functions, thus providing constraints to the dynamical susceptibility in linear response theory and the quantum Fisher information in quantum metrology.

III. QSL ON AUTOCORRELATION FUNCTIONS

Solving the dynamics of an arbitrary many-body quantum system is generally a demanding task. In many-body physics, the central objects that characterize the dynamics, determining for example the linear response [61], are the two-point time-correlation functions, whose explicit form is generally unknown. In particular, the so-called autocorrelation function

$$C_O(t) = \text{Tr}(O_t^\dagger O_0 \rho) \quad (17)$$

determines the operator growth of O_0 in Krylov space and therefore accounts for the build-up of the corresponding notion of operator complexity [57–60, 68].

Our QSLs on operators provide easily computable lower bounds to these quantities. In the following, we take O_0 to be Hermitian, ρ to be a stationary state, $[\rho, H] = 0$, and the Hamiltonian H to be time independent. In practical applications, ρ is often chosen to be the Gibbs state $e^{-\beta H}/Z$ at inverse temperature β , with $Z = \text{Tr} e^{-\beta H}$, but this assumption is not necessary for the derivation of the results below. Now, let us note that this autocorrelation function can be rewritten as the Hilbert-Schmidt inner product

$$C_O(t) = \langle \tilde{O}_t, \tilde{O}_0 \rangle \quad (18)$$

between a non-Hermitian operator \tilde{O}_0 and its time-evolved operator \tilde{O}_t , defined as follows:

$$\tilde{O}_0 \equiv O_0 \sqrt{\rho}, \quad \tilde{O}_t = U^\dagger \tilde{O}_0 U = O_t \sqrt{\rho}. \quad (19)$$

By making the commutator explicit and using that $[\rho, H] = 0$, we obtain $\| [H, \tilde{O}_0] \|^2 = \hbar^2 \langle \dot{O}_t^2 \rangle$, where the brackets stand for the expectation value with respect to ρ . We note that this characteristic velocity of the operator flow is time independent and thus does not require computing O_t . Being $\|\tilde{O}_0\|^2 = C_O(0)$ the norm of \tilde{O}_t , the autocorrelation function becomes $C_O(t) = C_O(0) \langle \tilde{O}_t | \tilde{O}_0 \rangle$. Substituting these expression into Eqs. (11) and (14), we can recast our MT QSL as a lower bound on the symmetrized autocorrelation function

$$\text{Re } C_O(t) = \frac{1}{2} \langle \{O_t, O_0\} \rangle \geq C_O(0) - \frac{1}{2} \langle \dot{O}_t^2 \rangle |_{t=0} t^2, \quad (20)$$

which, as also occurs for the decay of the state fidelity, corresponds to a short-time Taylor expansion up to second order. This early timescale was also identified in [69] and found to be proportional to the equilibration timescale at late times. While the MT QSL accounts for the short-time quadratic decay of the autocorrelation function, the ML QSL (16) yields instead a linear decay,

$$\text{Re } C_O(t) \geq C_O(0) - \frac{\alpha}{\hbar} \langle O_0 \{H - E_0, O_0\} \rangle t, \quad (21)$$

which identifies a new timescale. Again, as for the evolution of the operator overlap, we observe a crossover between the MT and the ML regimes, occurring at time

$$\tau_c = \frac{2\alpha}{\hbar} \frac{\langle O_0 \{H - E_0, O_0\} \rangle}{\langle \dot{O}_t^2 \rangle |_{t=0}}, \quad (22)$$

which is illustrated explicitly in Figs. 1 and 3 for a two-level system and a random matrix Hamiltonian, respectively.

Furthermore, as the operator dynamics is governed by the full autocorrelation function (17), one wishes to have a bound also on the anti-symmetrized, imaginary autocorrelation function $\langle [O_t, O_0] \rangle_0$. This quantity determines the linear response of the operator when the Hamiltonian is perturbed with an external, time-dependent driving [61]. Let us then discuss a ML-type upper bound on the imaginary part of the autocorrelation function. This can be achieved by noting that the imaginary part of the operator overlap (5) is upper bounded by the averaged Liouvillian $\langle |\mathbb{L}| \rangle$,

$$|\text{Im } \langle \tilde{O}_0 | \tilde{O}_t \rangle| = \frac{1}{2} |\langle [O_t, O_0] \rangle_0| \leq \langle |\mathbb{L}| \rangle t, \quad (23)$$

as one can see by using that $-|x| \leq \sin x \leq |x| \forall x$. Now, being $\text{Im } C_O(t) = -C_O(0) \text{Im } \langle \tilde{O}_0 | \tilde{O}_t \rangle$, we derive

$$|\text{Im } C_O(t)| \leq \langle O_0^\dagger \{H - E_0, O_0\} \rangle \frac{t}{\hbar}. \quad (24)$$

This result will be used below to derive analogous bounds on the linear response under an external perturbation and the thermal quantum Fisher information associated with an arbitrary observable O .

A. The two-level system

Before considering further applications of our results, let us analyze a simple model for which we can compute both the bounds (20)-(22) and the actual autocorrelation function $C_O(t)$, thus illustrating explicitly the existence of the aforementioned crossover.

Let us consider a two-level Hamiltonian

$$H = k \mathbb{1} + \vec{r} \cdot \vec{\sigma}, \quad (25)$$

where $\vec{\sigma} = (\sigma_x, \sigma_y, \sigma_z)$ is the Pauli matrix vector and $\vec{r} = (a, b, c)$. Let us choose $O_0 = \sigma_x$ as the initial operator and $\rho = e^{-\beta H}/Z$ as the state of the system. Then,

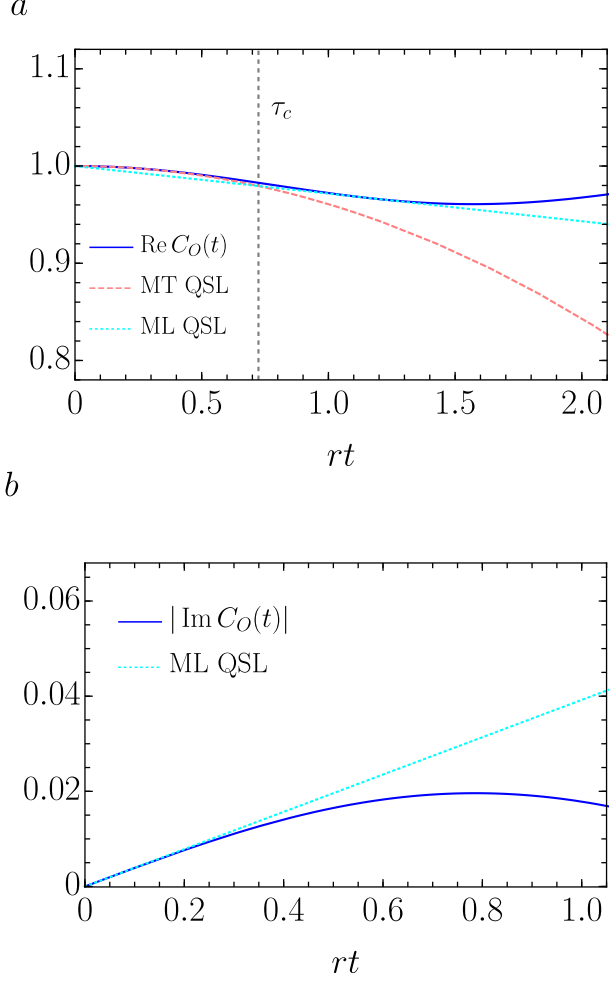


FIG. 1. Comparison of the real (a) and imaginary (b) parts of the correlation function with the MT and ML QSLs given by Eqs. (20), (21) and (24) for a two-level system. The parameters are chosen to be $a = 10$, $c = b = 1$ and the inverse temperature is $\beta = 10$. The identity in the Hamiltonian (25) plays no role, so we can fix $k = 0$ without loss of generality. (a) The initial decay of the symmetric correlation function undergoes a crossover from a regime dominated by the MT QSL to a regime in which the ML QSL becomes tighter. The vertical line corresponds to the crossover time τ_c . (b) The onset of the antisymmetric contribution is characterized by the ML QSL at short times.

using natural units $\hbar = 1$, the symmetric autocorrelation function is given by

$$\text{Re } C_O(t) = \frac{a^2 + (b^2 + c^2) \cos 2rt}{r^2}, \quad (26)$$

where $r \equiv |\vec{r}| = \sqrt{a^2 + b^2 + c^2}$, the temperature dependence being contained only in the antisymmetric part

$$\text{Im } C_O(t) = \frac{b^2 + c^2}{r^2} \tanh \beta r \sin 2rt. \quad (27)$$

Moreover, the MT and ML time scales have the following

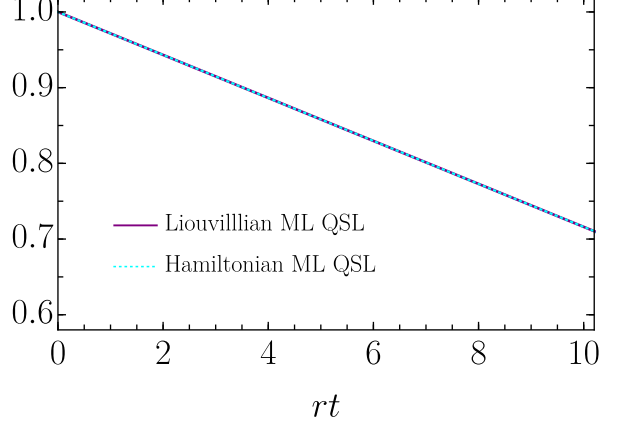


FIG. 2. The Liouvillian (10) and Hamiltonian (16) formulations of the ML bound for a two-level system are shown to be equivalent in the time window of interest. The parameters are chosen to be $a = 10$, $c = b = 1$ and the inverse temperature is $\beta = 10$.

expressions, respectively,

$$\langle \hat{O}_t^2 \rangle = 4(b^2 + c^2) \quad (28)$$

and

$$\langle O_0 \{ H - E_0, O_0 \} \rangle = \frac{2}{r} \left(\frac{2a^2}{1 + e^{2\beta r}} + b^2 + c^2 \right). \quad (29)$$

These can be inserted into Eqs. (20) and (21) to compute lower bounds on $\text{Re } C_O(t)$ and $\text{Im } C_O(t)$, as shown in Fig. 1. The symmetric, real part is the only nonvanishing term at the initial time and undergoes a decay, in parallel with the onset of the antisymmetric, imaginary contribution. This decay is initially captured by the MT QSL, as expected from Taylor expansion, while after the crossover time τ_c the ML QSL becomes tighter.

Finally, let us note that, for the parameters chosen ($a = 10$, $c = b = 1$ and $\beta = 10$), the two ML QSLs, formulated in terms either of the Hamiltonian (16) or the Liouvillian (10), are equivalent, as shown in Fig. 2. Indeed, in the latter case, the velocity is given by

$$C_O(0) \langle \tilde{O} | |\mathbb{L}| | \tilde{O} \rangle = \frac{2}{r} (b^2 + c^2), \quad (30)$$

so that the difference between the two ML velocities is

$$\frac{4a^2}{r} \frac{\alpha}{1 + e^{2\beta r}} \ll 1. \quad (31)$$

However, if one increases the temperature sufficiently the Liouvillian bound gives a tighter result.

B. Random matrix example

As already stressed, the above scenario consisting of an early quadratic decay governed by MT (20), a crossover,

and a subsequent time window in which ML (21) becomes tighter, proves to be a general feature of autocorrelations in isolated quantum systems. We further illustrate this feature in a generic setting, by sampling both the Hamiltonian and the initial operator (in the energy eigenbasis) from the Gaussian Orthogonal Ensemble (GOE) with standard deviation $\sigma = 1$ and dimension $d = 200$. The comparison between the autocorrelation function and the speed limits is shown in Fig. 3.

While the tangent character of the ML QSL to the real curve after the crossover is a feature specific to the qubit case (see Fig. 1), we observe that the divergence of the bound does not keep increasing when considering an increasing Hilbert space dimension. ML-type bounds were recently found to loose tightness for higher dimensions than a qubit also in [66].

IV. DYNAMICAL SUSCEPTIBILITIES

Thermal correlation functions determine the non-equilibrium response of an observable at the first order in the perturbation [61, 70]. Therefore, the results illustrated in the previous section allow us to bound the linear response, and, in particular, the dynamical susceptibility, which is the quantity that characterizes the response of a system to an external perturbation.

Let us then consider the situation in which a time-independent Hamiltonian H_0 is perturbed with an external, time-dependent driving,

$$H(t) = H_0 + \lambda V f(t), \quad (32)$$

where the perturbation operator V does not depend explicitly on time, λ is a real positive constant that quantifies the strength of the perturbation and the driving force $f(t)$, which can be taken to be $|f| \leq 1$, is assumed to vanish for $t \leq 0$. Let the initial state of the system be the thermal Gibbs state ρ_0 , relative to the unperturbed Hamiltonian H_0 , at inverse temperature β . We are interested in determining the linear response of an observable A , namely the shift of its expectation value at time t from the initial equilibrium value, $\langle A \rangle_t - \langle A \rangle_0$, where

$$\langle A \rangle_0 = \text{Tr}(A \rho_0), \quad \langle A \rangle_t = \text{Tr}[\rho_I(t) A_I(t)]. \quad (33)$$

Here, the operators are evaluated in the interaction picture

$$A_I(t) = U_0^\dagger(t) A U_0(t), \quad \rho_I(t) = U_V(t) \rho_0 U_V^\dagger(t), \quad (34)$$

with

$$U_0(t) = e^{-i H_0 \frac{t}{\hbar}}, \quad U_V(t) = \mathcal{T} e^{-i \frac{\lambda}{\hbar} \int_0^t V_I(s) f(s) ds}. \quad (35)$$

To the first order in λ , the linear response is given by the celebrated Kubo formula [61]

$$\langle A \rangle_t - \langle A \rangle_0 \simeq -i \frac{\lambda}{\hbar} \int_0^t \langle [A_I(t-s), V_I(0)] \rangle_0 f(s) ds. \quad (36)$$

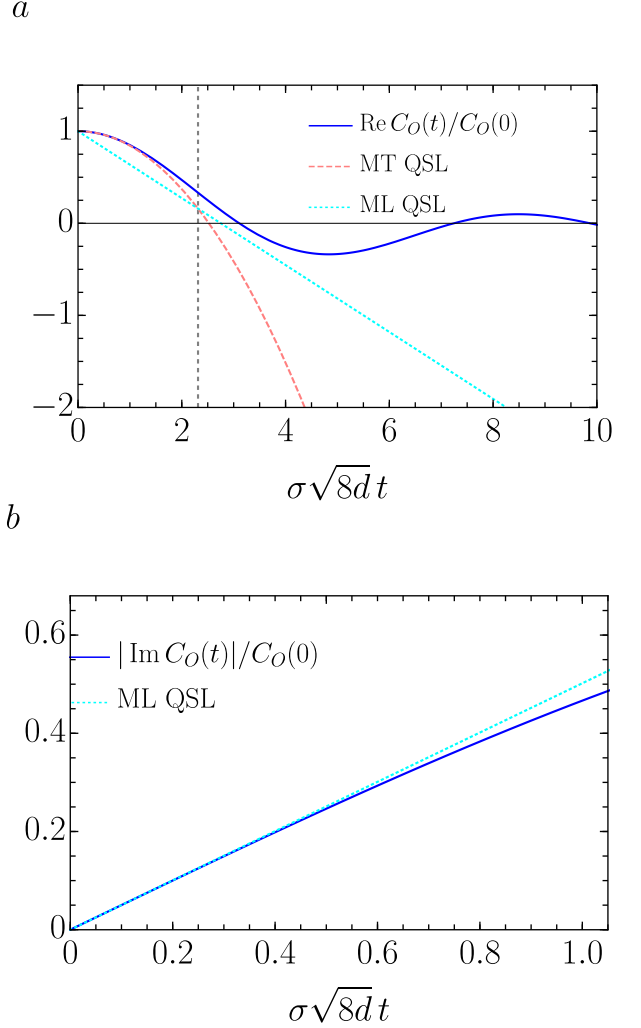


FIG. 3. Comparison of the real (a) and imaginary (b) parts of the (normalized) correlation function with the MT and ML QSLs given by Eqs. (20), (21) and (24), for $H, O_0 \in$ GOE with standard deviation $\sigma = 1$ and dimension $d = 200$. The QSLs have been here normalized dividing by $C_0(0)$. (a) The initial decay of the symmetric correlation function undergoes a crossover from a regime dominated by the MT QSL to a regime in which the ML QSL becomes tighter. The vertical line corresponds to the crossover time τ_c . (b) The onset of the antisymmetric contribution is characterized by the ML QSL at short times.

Thus, the non-equilibrium response, at the linear order, is determined by an equilibrium correlation function. As already stressed above, computing correlation functions at all times is generally a challenging task, equivalent to solving the dynamics. Therefore, having universal, model-independent bounds on these quantities is extremely useful. We next present several ways in which one can bound the right-hand side of Eq. (36).

The linear response (36) can be rewritten in terms of

the so-called dynamical susceptibility

$$\chi_{AV}(t) = -i\frac{1}{\hbar}\theta(t)\langle[A_I(t), V_I(0)]\rangle_0, \quad (37)$$

where $\theta(t)$ is the Heaviside function, as

$$\langle A \rangle_t - \langle A \rangle_0 = \lambda \int_{-\infty}^{\infty} \chi_{AV}(t-s)f(s)ds. \quad (38)$$

The dynamical susceptibility $\chi_{AV}(t)$, which vanishes for negative argument (i.e., before the external perturbation is applied), expresses the causal linear response of the system and is a real quantity. Its absolute value can be upper bounded using the Heisenberg uncertainty relation $|\langle [A, V] \rangle| \leq 2\Delta A \Delta V$, which yields the constant bound

$$|\chi_{AV}(t)| \leq \frac{2}{\hbar}\theta(t)\Delta_0 A \Delta_0 V, \quad (39)$$

where $\Delta_0^2 A$ is the variance with respect to ρ_0 . As the latter is time-independent in the interaction picture, we drop the subscript I . Alternatively, one can apply the Bogoliubov inequality [71]

$$|\langle [A, V] \rangle_0|^2 \leq \frac{\langle A^2 \rangle_0 \langle [V, [H_0, V]] \rangle_0}{k_B T}. \quad (40)$$

This yields a different upper bound with an explicit dependence on the temperature T

$$|\chi_{AV}(t)| \leq \frac{2\theta(t)}{\hbar} \sqrt{\frac{T}{T_B}} \Delta_0 V \Delta_0 A, \quad (41)$$

where we have defined the characteristic temperature

$$T_B \equiv \frac{\langle A^2 \rangle_0 \langle [V, [H_0, V]] \rangle_0}{4k_B(\Delta_0 A \Delta_0 V)^2}. \quad (42)$$

We see that at low temperature $T \leq T_B$ the Bogoliubov bound (41) is tighter than the Heisenberg bound (39), while the contrary holds at higher temperatures.

In certain experimental settings, one may be interested in quantifying the response of the perturbation operator V itself. For example, this is the case of the magnetic susceptibility in magnetic resonance experiments, where both V and the observable of interest A are given by the magnetization [72]. In such case, being $A = V$, the dynamical susceptibility $\chi_{VV}(t)$ becomes proportional to the anti-symmetrized autocorrelation function $\langle [V_I(t), V_I(0)] \rangle_0 = 2i \text{Im} C_V(t)$, and therefore one can make use of the techniques that we have illustrated above to bound autocorrelation functions by means of QSLs for operators. The ML QSL (22) yields the following upper bound on the dynamical susceptibility

$$|\chi_{VV}(t)| \leq \frac{t}{\tau_{QSL}^3} 2\theta(t)\hbar, \quad (43)$$

where we have introduced a new time scale $\tau_{QSL} = \hbar \langle V \{H_0 - E_0, V\} \rangle_0^{-1/3}$. Unlike the previous bounds (39)

and (41), Eq. (43) contains an explicit linear dependence on time. This implies that the QSL approach is the most efficient at early enough times. However, as we let the system evolve in time, the QSL bound (43) no longer governs the dynamics and one needs to consider different approaches. In particular, at lower temperature $T \leq T_B$, the QSL bound (43) ceases to be the tightest one at the time

$$\tau_B = \left(\frac{\Delta_0 V}{\hbar}\right)^2 \sqrt{\frac{T}{T_B}} \tau_{QSL}^3 \quad (44)$$

and for $t \geq \tau_B$ the Bogoliubov bound (41) gives the better description. By contrast, at high temperatures $T \geq T_B$, the crossover is between the QSL bound and the Heisenberg bound (39) and it occurs at time

$$\tau_H = \left(\frac{\Delta_0 V}{\hbar}\right)^2 \tau_{QSL}^3. \quad (45)$$

The bounds (39), (41) and (43) find applications in many experimentally relevant settings [72], of which we give two concrete examples below.

A. Examples

The situation in which a system is subject to an external perturbation is widespread in physics. A paradigmatic example is that of a system composed of N charged particles and perturbed with a uniform, time-dependent electric field $\vec{E}(t)$ [72]. In this case, the preferred observable to characterize the response of the system is the current flow \vec{J} and the corresponding dynamical susceptibility is the electrical conductivity. The perturbed Hamiltonian takes the form

$$H(t) = H_0 - \vec{R} \cdot \vec{E}(t), \quad (46)$$

where \vec{R} is the electric dipole moment in the origin

$$\vec{R} \equiv \sum_n q_n \vec{r}_n, \quad (47)$$

with q_n and \vec{r}_n being the charge and the position of the n -th particle. The net current vanishes at equilibrium, $\langle \vec{J} \rangle_0 = 0$, and the perturbed expectation value of the i -th spatial component J_i at time $t \geq 0$ is expressed, at the linear order, as [72]

$$\langle J_i \rangle_t = \sum_j \int_{-\infty}^{\infty} \sigma_{ij}(t-s) E_j(s) ds, \quad (48)$$

where $\sigma_{ij} \equiv \chi_{J_i R_j}$ is the electrical conductivity tensor. By using the bounds (39) and (41) we are able to derive the following constraints on σ_{ij} :

$$|\sigma_{ij}(t)| \leq \frac{2}{\hbar} \theta(t) \Delta_0 J_i \Delta_0 R_j, \quad (49)$$

$$|\sigma_{ij}(t)| \leq \frac{\theta(t)}{\hbar} \sqrt{\frac{\langle J_i^2 \rangle_0 \langle [R_j, [H_0, R_j]] \rangle_0}{k_B T}}. \quad (50)$$

Another experimental application in which the theory of linear response provides a useful approach is given by magnetic resonance experiments [73]. In this case, the central quantity is the magnetic susceptibility. Consider a paramagnetic system, initially aligned along a constant magnetic field \vec{B} and subsequently perturbed with a weak time-dependent field $\vec{h}(t)$, so that the total Hamiltonian reads

$$H(t) = -\vec{M} \cdot (\vec{B} + \vec{h}(t)). \quad (51)$$

The magnetization of the system is perturbed from its initial equilibrium value $\langle \vec{M} \rangle_0 = \chi_0 \vec{B}$, where χ_0 is the static susceptibility, and the linear response of its i -th component can be expressed using the Kubo formula

$$\langle M_i \rangle_t - \langle M_i \rangle_0 = \sum_j \int_{-\infty}^{\infty} \chi_{M,ij}(t-s) h_j(s) ds, \quad (52)$$

where $\chi_{M,ij}(t) \equiv \chi_{M_i M_j}(t)$ is the magnetic susceptibility tensor. The bounds (39) and (41) now yield

$$|\chi_{M,ij}(t)| \leq \frac{2}{\hbar} \theta(t) \Delta_0 M_i \Delta_0 M_j, \quad (53)$$

$$|\chi_{M,ij}(t)| \leq \frac{\theta(t)}{\hbar} \sqrt{\frac{\langle M_i^2 \rangle_0 \langle [M_j, [H_0, M_j]] \rangle_0}{k_B T}}. \quad (54)$$

Moreover, the diagonal magnetic susceptibilities can be upper bounded through the QSL approach (43) to find

$$|\chi_{M,ii}(t)| \leq \frac{2}{\hbar^2} \theta(t) \langle M_i^\dagger \{H_0 - E_0, M_i\} \rangle t. \quad (55)$$

V. BOUNDS ON THE QUANTUM FISHER INFORMATION

We next turn our attention to the application of QSL on operator flows in quantum metrology. In this context, the quantum Fisher information F_Q associated with a Hermitian operator O quantifies the maximal precision with which we can estimate the phase θ that parameterizes the *unitary flow*, of a given quantum state ρ , generated by the operator O . In other words, F_Q measures the distinguishability of the “initial” state ρ_0 from the one transformed by the unitary flow

$$\rho_\theta = e^{-i\theta O} \rho_0 e^{i\theta O}. \quad (56)$$

Let us note the change in the perspective: instead of looking at the *time* unitary flow that the observable O of interest undergoes under the action of the Hamiltonian that generates the dynamics, we are now considering the unitary flow (in a different parameter θ) of a given quantum state ρ under the action of O , that generates the state transformation. Remarkably, these two approaches are closely related, as the dynamical susceptibility χ_{OO} obtained using the first framework can be related to the quantum Fisher information F_Q [63, 74].

More precisely, for a thermal state ρ at temperature T , the following result on the quantum Fisher information has been shown by Hauke *et. al* in [63]

$$F_Q(T) = -\frac{4}{\pi} \int_0^\infty d\omega \tanh\left(\frac{\hbar\omega}{2k_B T}\right) \text{Im } \tilde{\chi}_{OO}(\omega, T), \quad (57)$$

where $\tilde{\chi}_{OO}(\omega, T)$ is the Fourier-transformed dynamical susceptibility, defined as

$$\tilde{\chi}_{OO}(\omega, T) = \int_0^\infty e^{i\omega t} \chi_{OO}(t, T) dt, \quad (58)$$

with $\chi_{OO}(t, T)$ being defined in Eq. (37) for $A = V = O$.

Now, the upper bound (24) we have derived above on the anti-symmetrized autocorrelation function $\text{Im } C_O$, together with the result (57), provides an upper bound on the quantum Fisher information F_Q . To this end, let us reverse the order of the integrals in Eq. (57) and perform first the one in ω . Computing the inverse Fourier transform of $\tanh(\omega/2T)$ and using the fact that $\chi_{OO}(t, T) = 2\theta(t) \text{Im } C_O(t, T)$ yields

$$F_Q(T) = -\frac{16k_B T}{\hbar} \int_0^\infty dt \operatorname{csch}\left(\pi k_B T \frac{t}{\hbar}\right) \text{Im } C_O(t, T). \quad (59)$$

Therefore, using that $\int_0^\infty dx x \operatorname{csch}(\pi q x) = (8q^2)^{-1} \forall q > 0$, from our previous result (24) we derive the following upper bound on the temperature-dependent quantum Fisher information

$$|F_Q(T)| \leq \frac{4}{k_B T} \langle O \{H - E_0, O\} \rangle, \quad (60)$$

where O is the operator that generates the transformation whose parameter is to be estimated, H is the Hamiltonian of the system and the expectation value is taken with respect to the corresponding thermal state at temperature T .

Let us finally note that, in this framework, the standard bounds (39) and (41) given by the Heisenberg and Bogoliubov inequalities are divergent, due to the divergence of $\operatorname{csch}(x)$ for $x \rightarrow 0$. Conversely, the time-linear dependence introduced by the QSL approach guarantees the convergence of the integral, yielding a finite upper bound on the quantum Fisher information. Making use of the celebrated Cramer-Rao bound $(\Delta\theta)^2 \geq (MF_Q)^{-1}$, Eq. (60) results in a lower bound on the variance of the parameter θ for M independent measurements

$$(\Delta\theta)^2 \geq \frac{k_B T}{4} \frac{1}{\langle O \{H - E_0, O\} \rangle}. \quad (61)$$

The precision can be enhanced by decreasing the temperature and by considering operators that develop stronger autocorrelations, since these lower bound (e.g., through Eq.(22)) the thermal correlation function $\langle O \{H - E_0, O\} \rangle$ appearing at the denominator.

VI. DISCUSSION

Conventional QSLs identify the minimum time scale in which a process can unfold by exploiting the notion of quantum state distinguishability. Yet, many applications in theoretical and experimental physics are naturally formulated in terms of operator flows. We have generalized the notion of QSL to this setting, providing bounds to the rate of unitary flows described by the conjugation of an observable by a one-parameter unitary.

Making use of Liouville space, we have derived analogs of the MT and ML QSLs, in which the minimum shift of the parameter required to distinguish the evolving operator from the initial one is lower bounded in terms of the mean and variance of the Liouvillian. These bounds generally exhibit a crossover, that we have characterized, and that is analogous to that observed in recent experiments for conventional QSLs.

We have also shown that QSLs for operator flows constrain the time-dependence of autocorrelation functions and thus the dynamic susceptibilities introduced in linear response theory to describe transport coefficients. In the context of quantum parameter estimation, we have shown that QSLs for operator flows yield bounds on the quantum Fisher information that restricts the estimation error through the Cramer-Rao bound. This last application makes explicit the fact that the flow under consideration need not be on time, but can describe shifts of an arbitrary parameter through a continuous symmetry. The situation is thus analogous to the generalization of uncertainty relations for quantum states [75].

Our results should find broad applications in nonequilibrium physics and, in particular, quantum technologies, including quantum metrology, quantum thermodynamics, and quantum computation. As we have demonstrated by several examples, our results are also of relevance in condensed matter physics to bound response functions and transport coefficients. We expect further applications of our results in other scenarios where operator flows naturally arise, such as the formulation of integrable systems in terms of Lax pairs and the Wegner renormalization group.

VII. AKNOWLEDGEMENTS

It is a pleasure to acknowledge discussions with Pablo Martínez-Azcona, Norman Margolus, Jing Yang, Apolonas S. Matsoukas-Roubeas and Silvia Pappalardi.

Appendix A: Deriving QSLs through a trigonometric approach

In this appendix we show an alternative derivation that results into two weaker QSLs on the operator overlap, proportional to the tighter QSLs (10) and (11) derived

in the main text. Making use of the trigonometric inequality

$$\cos x \geq 1 - \frac{2}{\pi}x - \frac{2}{\pi} \sin x, \quad (\text{A1})$$

valid for $x > 0$, we obtain

$$\begin{aligned} \text{Re} \langle O_0 | O_t \rangle &= \frac{1}{\|O\|^2} \sum_{j>k} \cos\left(\frac{\Delta_{jk}t}{\hbar}\right) (|O_{jk}|^2 + |O_{kj}|^2) \geq \\ &\geq \frac{1}{\|O\|^2} \sum_{j>k} \left(1 - \frac{2}{\pi} \frac{\Delta_{jk}t}{\hbar} - \frac{2}{\pi} \sin \frac{\Delta_{jk}t}{\hbar}\right) (|O_{jk}|^2 + |O_{kj}|^2). \end{aligned}$$

Therefore, being $\sin x \leq x$ for $x \geq 0$, we find

$$\text{Re} \langle O_0 | O_t \rangle \geq 1 - \frac{4}{\pi} \langle |\mathbb{L}| \rangle t, \quad (\text{A2})$$

that is,

$$t \geq \frac{\pi}{4} \frac{1 - \text{Re} \langle O_0 | O_t \rangle}{\langle |\mathbb{L}| \rangle} = \frac{\pi}{4} \frac{1 - \cos \mathcal{L}_t}{\langle |\mathbb{L}| \rangle}, \quad (\text{A3})$$

which is proportional to the ML QSL (10) derived in the main text through a constant smaller than one. Next, let us make use of the trigonometric inequality

$$\cos x \geq 1 - \frac{4}{\pi^2}x \sin x - \frac{2}{\pi^2}x^2, \quad (\text{A4})$$

which holds again $\forall x$. Combining it with the bound (7) on $\text{Re} \langle O_0 | \dot{O}_t \rangle$, we obtain

$$\begin{aligned} \text{Re} \langle O_0 | O_t \rangle &\geq \frac{1}{\|O\|^2} \sum_{j,k} |O_{jk}|^2 \left[1 - \frac{4}{\pi^2} \frac{\Delta_{jk}t}{\hbar} \sin \frac{\Delta_{jk}t}{\hbar} - \right. \\ &\quad \left. \frac{2}{\pi^2} \left(\frac{\Delta_{jk}t}{\hbar}\right)^2\right] = 1 + \frac{4}{\pi^2} \text{Re} \langle O_0 | \dot{O}_t \rangle t - \frac{2}{\pi^2} (\Delta \mathbb{L})^2 t^2 \geq \\ &\geq 1 - \frac{6}{\pi^2} (\Delta \mathbb{L})^2 t^2, \end{aligned}$$

that is,

$$t \geq \frac{\pi}{\sqrt{6}} \frac{\sqrt{1 - \text{Re} \langle O_0 | O_t \rangle}}{\Delta \mathbb{L}} = \frac{\pi}{\sqrt{6}} \frac{\sqrt{1 - \cos \mathcal{L}_t}}{\Delta \mathbb{L}}. \quad (\text{A5})$$

As for the case of ML, this bound is proportional to our MT QSL (11) for operators through a constant smaller than one, thus yielding a weaker result.

Appendix B: QSLs in the Schrödinger picture

In this appendix, we reformulate our results on operator flows in the context of the standard time-evolution of quantum states and compare them with the well-known MT [1] and ML [2] bounds. In this way, we provide a further justification for the bounds (11) and (10) to be regarded as generalizations of the MT and ML quantum speed limits to operator flows, respectively. To this end,

let us choose the initial operator O_0 to be the projector onto the pure state $|\psi_0\rangle$, $O_0 = |\psi_0\rangle\langle\psi_0|$, and let the expansion of $|\psi_0\rangle$ in the energy eigenbasis be

$$|\psi_0\rangle = \sum_j c_j |j\rangle, \quad (\text{B1})$$

where $H|j\rangle = E_j|j\rangle$ and $\sum_j |c_j|^2 = 1$. Then, the vectorization of O_0 is $|O_0\rangle = \sum_{jk} c_j^* c_k |j\rangle |k\rangle$, with $\|O_0\| = 1$. Since $|\psi_t\rangle = U_t |\psi_0\rangle$, where $U_t = e^{-iHt/\hbar}$, in order to reproduce the forward time-evolution of the quantum state we need to evolve the operator backwards in time:

$$O_{-t} = U_{-t}^\dagger O_0 U_{-t} = U_t |\psi_0\rangle\langle\psi_0| U_t^\dagger = |\psi_t\rangle\langle\psi_t|. \quad (\text{B2})$$

The operator overlap then reduces to the square modulus of the state overlap, that is, to the Uhlmann fidelity

$$\langle O_0 | O_{-t} \rangle = \text{Tr} \left(O_0^\dagger O_{-t} \right) = |\langle\psi_0|\psi_t\rangle|^2. \quad (\text{B3})$$

Moreover, being the Bures angle between states defined as

$$\ell_t = \arccos |\langle\psi_0|\psi_t\rangle|, \quad (\text{B4})$$

we have that $1 - \langle O_0 | O_{-t} \rangle = \sin^2 \ell_t$. We observe that the operator angle \mathcal{L}_t defined in Eq. (4) does not reduce to the standard Bures angle between states, being $\mathcal{L}_{-t} = \arccos |\langle\psi_0|\psi_t\rangle|^2$ when $O_0 = |\psi_0\rangle\langle\psi_0|$.

The typical maximal speeds of the flow, given by the ML (10) and MT (11) QSLs respectively, can be written as

$$\begin{aligned} \langle |\mathbb{L}| \rangle &= \frac{1}{\hbar} \sum_{jk} |\Delta_{jk}| |c_j|^2 |c_k|^2, \\ (\Delta \mathbb{L})^2 &= \frac{1}{\hbar^2} \sum_{jk} \Delta_{jk}^2 |c_j|^2 |c_k|^2. \end{aligned} \quad (\text{B5})$$

From the second equation, being also

$$(\Delta H)^2 = \sum_j E_j^2 |c_j|^2 - \sum_{jk} E_j E_k |c_j|^2 |c_k|^2, \quad (\text{B6})$$

we derive a proportionality relation between the Hamiltonian and Liouvillian variances (over $|\psi_0\rangle$ and $|O_0\rangle$, respectively):

$$(\Delta \mathbb{L})^2 = 2 \frac{(\Delta H)^2}{\hbar^2}. \quad (\text{B7})$$

Therefore, the MT bound (11) derived in the main text for operators reduces to the following QSL for states, given in terms of the energy variance:

$$t \geq \frac{\hbar}{\Delta H} \sin \ell_t. \quad (\text{B8})$$

In the case of orthogonal evolution $\langle\psi_0|\psi_\tau\rangle = 0$, we have $\sin \ell_\tau = 1$ and therefore we obtain a bound proportional

to (though weaker than) the standard Mandelstam-Tamm QSL [1],

$$\tau \geq \tau_{MT} = \frac{\pi \hbar}{2\Delta H} > \frac{\hbar}{\Delta H}, \quad (\text{B9})$$

thus justifying the interpretation of Eq. (11) as a MT-type of QSL for operators.

On the other hand, the mean energy can be rewritten as

$$\langle H \rangle = \sum_j E_j |c_j|^2 = \frac{1}{2} \sum_{jk} (E_j + E_k) |c_j|^2 |c_k|^2, \quad (\text{B10})$$

which, by using that $|\Delta_{jk}| = |E_j - E_k| \leq E_j + E_k - 2E_0$, implies

$$\langle |\mathbb{L}| \rangle \leq 2 \frac{\langle H \rangle - E_0}{\hbar}. \quad (\text{B11})$$

Therefore, we can recast the bound (10) as

$$t \geq \frac{\hbar}{2\alpha} \frac{\sin^2 \ell_t}{\langle H \rangle - E_0}, \quad (\text{B12})$$

which represents a generalization of the ML QSL [2] to the case of arbitrary angle between the initial and final states. A similar generalization was also claimed in reference [6], though their bound is not given in terms of $\langle H \rangle - E_0$, but rather in terms of the quantity $|\langle H \rangle|$. To our knowledge, the generalization of the ML bound to arbitrary angles between initial and final states was only proven numerically [16, 76, 77]. Let us note that, by considering again the orthogonalization time $t = \tau$, our QSL becomes

$$\tau \geq \tau_{ML} > \frac{\hbar}{2\alpha(\langle H \rangle - E_0)} \approx 0.44 \tau_{ML}, \quad (\text{B13})$$

where $\tau_{ML} = \pi\hbar/2(\langle H \rangle - E_0)$ is the well known ML QSL [2] for orthogonal evolution.

In conclusion, our bounds (10) and (11) on operator flows turn out to be proportional to the standard MT and ML QSLs for state evolution, justifying the given interpretation. The constant of proportionality is smaller than one, meaning that our bounds are not violated, though they are not tight for quantum state evolution.

Finally, let us perform a numerical test of our ML QSL for states (B12), which can be recast as a lower bound on the state overlap

$$|\langle\psi_0|\psi_t\rangle|^2 \geq 1 - 2\alpha(\langle H \rangle - E_0)t/\hbar. \quad (\text{B14})$$

In Fig. 4, we test the bound (B14) for a single realization of a random matrix Hamiltonian H of dimension $d = 50$, generated from the Gaussian Orthogonal Ensemble (GOE) with variance $\sigma = 1$. The initial state is chosen to be the coherent Gibbs state at inverse temperature β

$$|\psi_0\rangle = \frac{1}{\sqrt{Z}} \sum_{n=1}^d e^{-\beta \frac{E_n}{2}} |n\rangle, \quad (\text{B15})$$

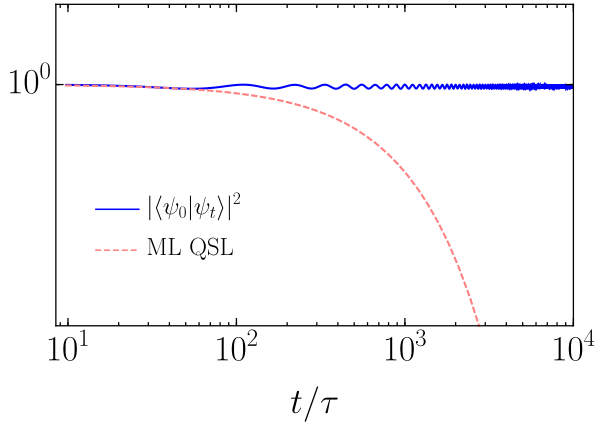


FIG. 4. The coherent Gibbs state overlap undergoes an initial decay which is qualitatively captured by the ML QSL for states (B14). The parameter chosen for the simulation are $\sigma = 1$, $d = 50$ and inverse temperature $\beta = 10$.

where $Z = \sum_n e^{-\beta E_n}$ is the partition function. In this setting, the quantum state overlap can be conveniently rewritten in terms of the analitically-continued partition function as follows [78, 79]

$$\langle \psi_0 | \psi_t \rangle = \frac{Z(\beta + it)}{Z(\beta)}. \quad (\text{B16})$$

After the initial decay shown in Fig. 4, the fidelity undergoes an oscillatory behavior that is no longer captured by the QSL (B14). Deviations from the bound appear far after the characteristic timescale $\tau = (\sigma\sqrt{8d})^{-1}$, where $\sigma\sqrt{8d}$ correspond to the width of the eigenvalue distribution (i.e., to the diameter of the Wigner semicircle law), that is to the largest frequency involved in the evolution.

Appendix C: Margolous-Levitin QSL on operator flows with driven Hamiltonians

Finally, we partially extend our results to the case in which the Hamiltonian generating the unitary flow $O_t = U_t^\dagger O_0 U_t$ is time dependent, that is

$$U_t = \mathcal{T} \exp -\frac{i}{\hbar} \int_0^t H(s) ds. \quad (\text{C1})$$

We focus on the case in which O_0 is an observable, i.e., a Hermitian operator. Moreover, let us assume that the Hamiltonians at different times commute, so that we can drop the time-ordering operator \mathcal{T} in front of the exponential. In addition, if we make the strongest assumption that H_t remains diagonal in the initial eigenbasis,

$$H_t = \sum_j E_j(t) |j\rangle \langle j|, \quad (\text{C2})$$

where only the eigenvalues $E_j(t)$ depend on time, then we can write the action of U_t over the energy eigenvector $|j\rangle$ as

$$U_t |j\rangle = e^{-\frac{i}{\hbar} \int_0^t E_j(s) ds} |j\rangle. \quad (\text{C3})$$

Under this assumption, the operator overlap can be expanded as

$$\langle O_0 | O_t \rangle = \frac{1}{\|O\|^2} \sum_{j,k} e^{i \frac{\Delta_{jk}(t)}{\hbar} t} |O_{jk}|^2, \quad (\text{C4})$$

so that, making use of the inequality $\cos x \geq 1 - \alpha|x|$ [65] as in the main text, we derive a ML bound on operator flows in the case of driven dynamics,

$$t \geq \frac{1 - \text{Re} \langle O_0 | O_t \rangle}{\alpha \langle |L| \rangle} = \frac{1 - \cos \mathcal{L}_t}{\alpha \langle |L| \rangle}, \quad (\text{C5})$$

where $\bar{f}(t) = \frac{1}{t} \int_0^t f(u) du$ is the time average at time t . As a consequence, by choosing $O_0 = |\psi_0\rangle \langle \psi_0|$, we obtain a generalization of the ML QSL for state evolution under driven Hamiltonians and arbitrary angles:

$$t \geq \frac{\hbar}{2\alpha} \frac{\sin^2 \ell_t}{\langle H \rangle - E_0}, \quad (\text{C6})$$

valid when the energy eigenvectors are stationary. A related result was also claimed in reference [10], but their derivation was later shown to generalize the MT QSL rather than the ML one, as pointed out in [80].

[1] L. Mandelstam and I. Tamm. Quantum speed limits: from heisenberg's uncertainty principle to optimal quantum control. *J. Phys. USSR*, 9:249, 1945.

[2] Norman Margolus and Lev B. Levitin. The maximum speed of dynamical evolution. *Physica D: Non-linear Phenomena*, 120(1):188–195, 1998. ISSN 0167-2789. doi:[https://doi.org/10.1016/S0167-2789\(98\)00054-2](https://doi.org/10.1016/S0167-2789(98)00054-2). URL <https://www.sciencedirect.com/science/article/pii/S0167278998000542>. Proceedings of the Fourth Workshop on Physics and Consumption.

[3] Armin Uhlmann. An energy dispersion estimate. *Physics Letters A*, 161(4):329 – 331, 1992. ISSN 0375-9601. doi:[https://doi.org/10.1016/0375-9601\(92\)90555-Z](https://doi.org/10.1016/0375-9601(92)90555-Z). URL <http://www.sciencedirect.com/science/article/pii/S037596019290555Z>.

[article/doi/0375960192905552](https://doi.org/10.1103/article/doi/0375960192905552).

[4] Francesco Campaioli, Felix A. Pollock, Felix C. Binder, and Kavan Modi. Tightening quantum speed limits for almost all states. *Phys. Rev. Lett.*, 120:060409, Feb 2018. doi:10.1103/PhysRevLett.120.060409. URL <https://link.aps.org/doi/10.1103/PhysRevLett.120.060409>.

[5] J. Anandan and Y. Aharonov. Geometry of quantum evolution. *Phys. Rev. Lett.*, 65:1697–1700, Oct 1990. doi:10.1103/PhysRevLett.65.1697. URL <https://link.aps.org/doi/10.1103/PhysRevLett.65.1697>.

[6] Sebastian Deffner and Eric Lutz. Energy–time uncertainty relation for driven quantum systems. *Journal of Physics A: Mathematical and Theoretical*, 46(33):335302, jul 2013. doi:10.1088/1751-8113/46/33/335302. URL <https://doi.org/10.1088/1751-8113/46/33/335302>.

[7] Manaka Okuyama and Masayuki Ohzeki. Comment on ‘energy-time uncertainty relation for driven quantum systems’. *Journal of Physics A: Mathematical and Theoretical*, 51(31):318001, jun 2018. doi:10.1088/1751-8121/aacb90. URL <https://doi.org/10.1088/1751-8121/aacb90>.

[8] M. M. Taddei, B. M. Escher, L. Davidovich, and R. L. de Matos Filho. Quantum speed limit for physical processes. *Phys. Rev. Lett.*, 110:050402, Jan 2013. doi:10.1103/PhysRevLett.110.050402. URL <https://link.aps.org/doi/10.1103/PhysRevLett.110.050402>.

[9] A. del Campo, I. L. Egusquiza, M. B. Plenio, and S. F. Huelga. Quantum speed limits in open system dynamics. *Phys. Rev. Lett.*, 110:050403, Jan 2013. doi:10.1103/PhysRevLett.110.050403. URL <https://link.aps.org/doi/10.1103/PhysRevLett.110.050403>.

[10] Sebastian Deffner and Eric Lutz. Quantum speed limit for non-markovian dynamics. *Phys. Rev. Lett.*, 111:010402, Jul 2013. doi:10.1103/PhysRevLett.111.010402. URL <https://link.aps.org/doi/10.1103/PhysRevLett.111.010402>.

[11] Francesco Campaioli, Felix A. Pollock, and Kavan Modi. Tight, robust, and feasible quantum speed limits for open dynamics. *Quantum*, 3:168, August 2019. ISSN 2521-327X. doi:10.22331/q-2019-08-05-168. URL <https://doi.org/10.22331/q-2019-08-05-168>.

[12] Luis Pedro García-Pintos and Adolfo del Campo. Quantum speed limits under continuous quantum measurements. *New Journal of Physics*, 21(3):033012, mar 2019. doi:10.1088/1367-2630/ab099e. URL <https://doi.org/10.1088/1367-2630/ab099e>.

[13] B. Shanahan, A. Chenu, N. Margolus, and A. del Campo. Quantum speed limits across the quantum-to-classical transition. *Phys. Rev. Lett.*, 120:070401, Feb 2018. doi:10.1103/PhysRevLett.120.070401. URL <https://link.aps.org/doi/10.1103/PhysRevLett.120.070401>.

[14] Manaka Okuyama and Masayuki Ohzeki. Quantum speed limit is not quantum. *Phys. Rev. Lett.*, 120:070402, Feb 2018. doi:10.1103/PhysRevLett.120.070402. URL <https://link.aps.org/doi/10.1103/PhysRevLett.120.070402>.

[15] Naoto Shiraishi, Ken Funo, and Keiji Saito. Speed limit for classical stochastic processes. *Phys. Rev. Lett.*, 121:070601, Aug 2018. doi:10.1103/PhysRevLett.121.070601. URL <https://link.aps.org/doi/10.1103/PhysRevLett.121.070601>.

[16] Sebastian Deffner and Steve Campbell. Quantum speed limits: from heisenberg’s uncertainty principle to optimal quantum control. *Journal of Physics A: Mathematical and Theoretical*, 50(45):453001, oct 2017. doi:10.1088/1751-8121/aa86c6. URL <https://doi.org/10.1088/1751-8121/aa86c6>.

[17] S. Lloyd. Ultimate physical limits to computation. *Nature*, 406(6799):1047–1054, 2000.

[18] Seth Lloyd. Computational capacity of the universe. *Phys. Rev. Lett.*, 88:237901, May 2002. doi:10.1103/PhysRevLett.88.237901. URL <https://link.aps.org/doi/10.1103/PhysRevLett.88.237901>.

[19] Vittorio Giovannetti, Seth Lloyd, and Lorenzo Maccone. Advances in quantum metrology. *Nature Photonics*, 5(4):222–229, 2011. ISSN 1749-4893. doi:10.1038/nphoton.2011.35. URL <https://doi.org/10.1038/nphoton.2011.35>.

[20] M. Beau and A. del Campo. Nonlinear quantum metrology of many-body open systems. *Phys. Rev. Lett.*, 119:010403, Jul 2017. doi:10.1103/PhysRevLett.119.010403. URL <https://link.aps.org/doi/10.1103/PhysRevLett.119.010403>.

[21] T. Caneva, M. Murphy, T. Calarco, R. Fazio, S. Montangero, V. Giovannetti, and G. E. Santoro. Optimal control at the quantum speed limit. *Phys. Rev. Lett.*, 103:240501, Dec 2009. doi:10.1103/PhysRevLett.103.240501. URL <https://link.aps.org/doi/10.1103/PhysRevLett.103.240501>.

[22] Gerhard C. Hegerfeldt. Driving at the quantum speed limit: Optimal control of a two-level system. *Phys. Rev. Lett.*, 111:260501, Dec 2013. doi:10.1103/PhysRevLett.111.260501. URL <https://link.aps.org/doi/10.1103/PhysRevLett.111.260501>.

[23] Ken Funo, Jing-Ning Zhang, Cyril Chatou, Kihwan Kim, Masahito Ueda, and Adolfo del Campo. Universal work fluctuations during shortcuts to adiabaticity by counter-diabatic driving. *Phys. Rev. Lett.*, 118:100602, Mar 2017. doi:10.1103/PhysRevLett.118.100602. URL <https://link.aps.org/doi/10.1103/PhysRevLett.118.100602>.

[24] Steve Campbell and Sebastian Deffner. Trade-off between speed and cost in shortcuts to adiabaticity. *Phys. Rev. Lett.*, 118:100601, Mar 2017. doi:10.1103/PhysRevLett.118.100601. URL <https://link.aps.org/doi/10.1103/PhysRevLett.118.100601>.

[25] Sahar Alipour, Aurelia Chenu, Ali T. Rezakhani, and Adolfo del Campo. Shortcuts to Adiabaticity in Driven Open Quantum Systems: Balanced Gain and Loss and Non-Markovian Evolution. *Quantum*, 4:336, September 2020. ISSN 2521-327X. doi:10.22331/q-2020-09-28-336. URL <https://doi.org/10.22331/q-2020-09-28-336>.

[26] Ken Funo, Neill Lambert, and Franco Nori. General bound on the performance of counter-diabatic driving acting on dissipative spin systems. *Phys. Rev. Lett.*, 127:150401, Oct 2021. doi:10.1103/PhysRevLett.127.150401. URL <https://link.aps.org/doi/10.1103/PhysRevLett.127.150401>.

[27] Marin Bukov, Dries Sels, and Anatoli Polkovnikov. Geometric speed limit of accessible many-body state preparation. *Phys. Rev. X*, 9:011034, Feb 2019. doi:10.1103/PhysRevX.9.011034. URL <https://link.aps.org/doi/10.1103/PhysRevX.9.011034>.

[28] Keisuke Suzuki and Kazutaka Takahashi. Performance evaluation of adiabatic quantum computation via quantum speed limits and possible applications to many-body systems. *Phys. Rev. Research*, 2:032016, Jul 2020. doi:10.1103/PhysRevResearch.2.032016. URL <https://link.aps.org/doi/10.1103/PhysRevResearch.2.032016>.

[PhysRevResearch.2.032016](https://doi.org/10.1103/PhysRevResearch.2.032016).

[29] Adolfo del Campo. Probing quantum speed limits with ultracold gases. *Phys. Rev. Lett.*, 126:180603, May 2021. doi:10.1103/PhysRevLett.126.180603. URL <https://link.aps.org/doi/10.1103/PhysRevLett.126.180603>.

[30] Ryusuke Hamazaki. Speed limits for macroscopic transitions. *arXiv:2110.09716*, 2021. URL <https://arxiv.org/abs/2110.09716>.

[31] Zongping Gong and Ryusuke Hamazaki. Bounds in nonequilibrium quantum dynamics. *arXiv:2202.02011*, 2022. URL <https://arxiv.org/abs/2202.02011>.

[32] Jun Jing, Lian-Ao Wu, and Adolfo del Campo. Fundamental speed limits to the generation of quantumness. *Scientific Reports*, 6(1):38149, Nov 2016. ISSN 2045-2322. doi:10.1038/srep38149. URL <https://doi.org/10.1038/srep38149>.

[33] Iman Marvian, Robert W. Spekkens, and Paolo Zanardi. Quantum speed limits, coherence, and asymmetry. *Phys. Rev. A*, 93:052331, May 2016. doi:10.1103/PhysRevA.93.052331. URL <https://link.aps.org/doi/10.1103/PhysRevA.93.052331>.

[34] Brij Mohan, Siddhartha Das, and Arun Kumar Pati. Quantum speed limits for information and coherence. *New Journal of Physics*, 24(6):065003, jun 2022. doi:10.1088/1367-2630/ac753c. URL <https://doi.org/10.1088/1367-2630/ac753c>.

[35] Francesco Campaioli, Chang shui Yu, Felix A Pollock, and Kavan Modi. Resource speed limits: maximal rate of resource variation. *New Journal of Physics*, 24(6):065001, jun 2022. doi:10.1088/1367-2630/ac7346. URL <https://doi.org/10.1088/1367-2630/ac7346>.

[36] Todd R. Gingrich, Jordan M. Horowitz, Nikolay Perunov, and Jeremy L. England. Dissipation bounds all steady-state current fluctuations. *Phys. Rev. Lett.*, 116:120601, Mar 2016. doi:10.1103/PhysRevLett.116.120601. URL <https://link.aps.org/doi/10.1103/PhysRevLett.116.120601>.

[37] Yoshihiko Hasegawa. Thermodynamic uncertainty relation for general open quantum systems. *Phys. Rev. Lett.*, 126:010602, Jan 2021. doi:10.1103/PhysRevLett.126.010602. URL <https://link.aps.org/doi/10.1103/PhysRevLett.126.010602>.

[38] Schuyler B. Nicholson, Luis Pedro García-Pintos, Adolfo del Campo, and Jason R. Green. Time-information uncertainty relations in thermodynamics. *Nature Physics*, 16(12):1211–1215, Dec 2020. ISSN 1745-2481. doi:10.1038/s41567-020-0981-y. URL <https://doi.org/10.1038/s41567-020-0981-y>.

[39] Van Tuan Vo, Tan Van Vu, and Yoshihiko Hasegawa. Unified approach to classical speed limit and thermodynamic uncertainty relation. *Phys. Rev. E*, 102:062132, Dec 2020. doi:10.1103/PhysRevE.102.062132. URL <https://link.aps.org/doi/10.1103/PhysRevE.102.062132>.

[40] Luis Pedro García-Pintos, Schuyler B. Nicholson, Jason R. Green, Adolfo del Campo, and Alexey V. Gorshkov. Unifying quantum and classical speed limits on observables. *Phys. Rev. X*, 12:011038, Feb 2022. doi:10.1103/PhysRevX.12.011038. URL <https://link.aps.org/doi/10.1103/PhysRevX.12.011038>.

[41] Brij Mohan and Arun Kumar Pati. Quantum speed limits for observable, 2021. URL <https://arxiv.org/abs/2112.13789>.

[42] Franz J. Wegner. Flow equations for hamiltonians. *Physics Reports*, 348(1):77–89, 2001. ISSN 0370-1573. doi:[https://doi.org/10.1016/S0370-1573\(00\)00136-8](https://doi.org/10.1016/S0370-1573(00)00136-8). URL <https://www.sciencedirect.com/science/article/pii/S0370157300001368>.

[43] Pablo M. Poggi. Geometric quantum speed limits and short-time accessibility to unitary operations. *Phys. Rev. A*, 99:042116, Apr 2019. doi:10.1103/PhysRevA.99.042116. URL <https://link.aps.org/doi/10.1103/PhysRevA.99.042116>.

[44] Raam Uzdin. Resources needed for non-unitary quantum operations. *Journal of Physics A: Mathematical and Theoretical*, 46(14):145302, mar 2013. doi:10.1088/1751-8113/46/14/145302. URL <https://doi.org/10.1088/2F1751-8113%2F46%2F14%2F145302>.

[45] Raam Uzdin and Ronnie Kosloff. Speed limits in liouville space for open quantum systems. *EPL (Europhysics Letters)*, 115(4):40003, aug 2016. doi:10.1209/0295-5075/115/40003. URL <https://doi.org/10.1209/0295-5075/115/40003>.

[46] C. W. von Keyserlingk, Tibor Rakovszky, Frank Pollmann, and S. L. Sondhi. Operator hydrodynamics, otocs, and entanglement growth in systems without conservation laws. *Phys. Rev. X*, 8:021013, Apr 2018. doi:10.1103/PhysRevX.8.021013. URL <https://link.aps.org/doi/10.1103/PhysRevX.8.021013>.

[47] Vedika Khemani, Ashvin Vishwanath, and David A. Huse. Operator spreading and the emergence of dissipative hydrodynamics under unitary evolution with conservation laws. *Phys. Rev. X*, 8:031057, Sep 2018. doi:10.1103/PhysRevX.8.031057. URL <https://link.aps.org/doi/10.1103/PhysRevX.8.031057>.

[48] Adam Nahum, Sagar Vijay, and Jeongwan Haah. Operator spreading in random unitary circuits. *Phys. Rev. X*, 8:021014, Apr 2018. doi:10.1103/PhysRevX.8.021014. URL <https://link.aps.org/doi/10.1103/PhysRevX.8.021014>.

[49] Sarang Gopalakrishnan, David A. Huse, Vedika Khemani, and Romain Vasseur. Hydrodynamics of operator spreading and quasiparticle diffusion in interacting integrable systems. *Phys. Rev. B*, 98:220303, Dec 2018. doi:10.1103/PhysRevB.98.220303. URL <https://link.aps.org/doi/10.1103/PhysRevB.98.220303>.

[50] Tibor Rakovszky, Frank Pollmann, and C. W. von Keyserlingk. Diffusive hydrodynamics of out-of-time-ordered correlators with charge conservation. *Phys. Rev. X*, 8:031058, Sep 2018. doi:10.1103/PhysRevX.8.031058. URL <https://link.aps.org/doi/10.1103/PhysRevX.8.031058>.

[51] Leonard Susskind. Computational complexity and black hole horizons. *Fortschritte der Physik*, 64(1):24–43, 2016. doi:<https://doi.org/10.1002/prop.201500092>. URL <https://onlinelibrary.wiley.com/doi/abs/10.1002/prop.201500092>.

[52] Adam R. Brown, Daniel A. Roberts, Leonard Susskind, Brian Swingle, and Ying Zhao. Holographic complexity equals bulk action? *Phys. Rev. Lett.*, 116:191301, May 2016. doi:10.1103/PhysRevLett.116.191301. URL <https://link.aps.org/doi/10.1103/PhysRevLett.116.191301>.

[53] Adam R. Brown, Daniel A. Roberts, Leonard Susskind, Brian Swingle, and Ying Zhao. Complexity, action, and black holes. *Phys. Rev. D*, 93:086006, Apr 2016. doi:10.1103/PhysRevD.93.086006. URL <https://link.aps.org/doi/10.1103/PhysRevD.93.086006>.

[org/doi/10.1103/PhysRevD.93.086006](https://doi.org/10.1103/PhysRevD.93.086006).

[54] Shira Chapman, Michal P. Heller, Hugo Marrochio, and Fernando Pastawski. Toward a definition of complexity for quantum field theory states. *Phys. Rev. Lett.*, 120:121602, Mar 2018. doi: 10.1103/PhysRevLett.120.121602. URL <https://link.aps.org/doi/10.1103/PhysRevLett.120.121602>.

[55] J. Molina-Vilaplana and A. del Campo. Complexity functionals and complexity growth limits in continuous mera circuits. *Journal of High Energy Physics*, 2018(8):12, Aug 2018. ISSN 1029-8479. doi:10.1007/JHEP08(2018)012. URL [https://doi.org/10.1007/JHEP08\(2018\)012](https://doi.org/10.1007/JHEP08(2018)012).

[56] Niklas Hörnedal, Nicoletta Carabba, Apollonas S. Matsoukas-Roubeas, and Adolfo del Campo. Ultimate physical limits to the growth of operator complexity. *arXiv:2202.05006*, 2022. URL <https://arxiv.org/abs/2202.05006>.

[57] Daniel E. Parker, Xiangyu Cao, Alexander Avdoshkin, Thomas Scaffidi, and Ehud Altman. A universal operator growth hypothesis. *Phys. Rev. X*, 9:041017, Oct 2019. doi:10.1103/PhysRevX.9.041017. URL <https://link.aps.org/doi/10.1103/PhysRevX.9.041017>.

[58] J.L.F. Barbón, E. Rabinovici, R. Shir, and R. Sinha. On the evolution of operator complexity beyond scrambling. *J. High Energ. Phys.*, 2019(10):264, October 2019. ISSN 1029-8479. doi:10.1007/JHEP10(2019)264. URL [https://doi.org/10.1007/JHEP10\(2019\)264](https://doi.org/10.1007/JHEP10(2019)264).

[59] E. Rabinovici, A. Sánchez-Garrido, R. Shir, and J. Sonner. Operator complexity: a journey to the edge of Krylov space. *J. High Energ. Phys.*, 2021(6):62, June 2021. ISSN 1029-8479. doi:10.1007/JHEP06(2021)062. URL [https://doi.org/10.1007/JHEP06\(2021\)062](https://doi.org/10.1007/JHEP06(2021)062).

[60] Paweł Caputa, Javier M. Magan, and Dimitrios Patramanis. Geometry of Krylov Complexity. *arXiv:2109.03824*, September 2021. URL [http://arxiv.org/abs/2109.03824](https://arxiv.org/abs/2109.03824). arXiv: 2109.03824.

[61] Ryogo Kubo. Statistical-mechanical theory of irreversible processes. i. general theory and simple applications to magnetic and conduction problems. *Journal of the Physical Society of Japan*, 12(6):570–586, 1957. doi: 10.1143/JPSJ.12.570. URL <https://doi.org/10.1143/JPSJ.12.570>.

[62] Gal Ness, Manolo R. Lam, Wolfgang Alt, Dieter Meschede, Yoav Sagi, and Andrea Alberti. Observing crossover between quantum speed limits. *Science Advances*, 7(52):eabj9119, 2021. doi: 10.1126/sciadv.abj9119. URL <https://www.science.org/doi/abs/10.1126/sciadv.abj9119>.

[63] Philipp Hauke, Markus Heyl, Luca Tagliacozzo, and Peter Zoller. Measuring multipartite entanglement through dynamic susceptibilities. *Nature Physics*, 12(8):778–782, 2016. doi:10.1038/nphys3700. URL <https://doi.org/10.1038/nphys3700>.

[64] Xiaoguang Wang, Zhe Sun, and Z. D. Wang. Operator fidelity susceptibility: An indicator of quantum criticality. *Phys. Rev. A*, 79:012105, Jan 2009. doi: 10.1103/PhysRevA.79.012105. URL <https://link.aps.org/doi/10.1103/PhysRevA.79.012105>.

[65] Ole Andersson. Holonomy in quantum information geometry. 2019.

[66] Gal Ness, Andrea Alberti, and Yoav Sagi. Quantum speed limit for states with a bounded energy spectrum, 2022. URL <https://arxiv.org/abs/2206.14803>.

[67] Lev B. Levitin and Tommaso Toffoli. Fundamental limit on the rate of quantum dynamics: The unified bound is tight. *Phys. Rev. Lett.*, 103:160502, Oct 2009. doi: 10.1103/PhysRevLett.103.160502. URL <https://link.aps.org/doi/10.1103/PhysRevLett.103.160502>.

[68] Anatoly Dymarsky and Michael Smolkin. Krylov complexity in conformal field theory. *Phys. Rev. D*, 104: L081702, Oct 2021. doi:10.1103/PhysRevD.104.L081702. URL <https://link.aps.org/doi/10.1103/PhysRevD.104.L081702>.

[69] Álvaro M. Alhambra, Jonathon Riddell, and Luis Pedro García-Pintos. Time evolution of correlation functions in quantum many-body systems. *Phys. Rev. Lett.*, 124:110605, Mar 2020. doi: 10.1103/PhysRevLett.124.110605. URL <https://link.aps.org/doi/10.1103/PhysRevLett.124.110605>.

[70] Mark E. Tuckerman. *Statistical Mechanics: Theory and Molecular Simulation*. Oxford University Press, 2010.

[71] Masahito Ueda. *Fundamentals and New Frontiers of Bose-Einstein Condensation*. WORLD SCIENTIFIC, 2010. doi:10.1142/7216. URL <https://www.worldscientific.com/doi/abs/10.1142/7216>.

[72] Gene F. Mazenko. *Time-Dependent Phenomena in Condensed-Matter Systems: Relationship Between Theory and Experiment*, chapter 2, pages 19–62. John Wiley Sons, 2006. ISBN 9783527618958. doi: <https://doi.org/10.1002/9783527618958.ch2>.

[73] G.E. Pake. *Paramagnetic Resonance: An Introductory Monograph*. Number v. 1 in Frontiers in physics. W.A. Benjamin, 1962. URL <https://books.google.lu/books?id=B8pEAAAIAAJ>.

[74] Marlon Brener, Silvia Pappalardi, John Goold, and Alessandro Silva. Multipartite entanglement structure in the eigenstate thermalization hypothesis. *Phys. Rev. Lett.*, 124:040605, Jan 2020. doi: 10.1103/PhysRevLett.124.040605. URL <https://link.aps.org/doi/10.1103/PhysRevLett.124.040605>.

[75] Samuel L. Braunstein, Carlton M. Caves, and G.J. Milburn. Generalized uncertainty relations: Theory, examples, and lorentz invariance. *Annals of Physics*, 247(1):135–173, 1996. ISSN 0003-4916. doi:<https://doi.org/10.1006/aphy.1996.0040>. URL <https://www.sciencedirect.com/science/article/pii/S0003491696900408>.

[76] Vittorio Giovannetti, Seth Lloyd, and Lorenzo Maccone. Quantum limits to dynamical evolution. *Phys. Rev. A*, 67:052109, May 2003. doi:10.1103/PhysRevA.67.052109. URL <https://link.aps.org/doi/10.1103/PhysRevA.67.052109>.

[77] Vittorio Giovannetti, Seth Lloyd, and Lorenzo Maccone. The speed limit of quantum unitary evolution. *Journal of Optics B: Quantum and Semiclassical Optics*, 6(8):S807–S810, jul 2004. doi:10.1088/1464-4266/6/8/028. URL <https://doi.org/10.1088/1464-4266/6/8/028>.

[78] A. del Campo, J. Molina-Vilaplana, and J. Sonner. Scrambling the spectral form factor: Unitarity constraints and exact results. *Phys. Rev. D*, 95:126008, Jun 2017. doi:10.1103/PhysRevD.95.126008. URL <https://link.aps.org/doi/10.1103/PhysRevD.95.126008>.

[79] Zhenyu Xu, Aurelia Chenu, Tomaž Prosen, and Adolfo del Campo. Thermofield dynamics: Quantum chaos versus decoherence. *Phys. Rev. B*, 103:064309, Feb 2021. doi:10.1103/PhysRevB.103.064309. URL <https://link.aps.org/doi/10.1103/PhysRevB.103.064309>.

[80] Manaka Okuyama, Ryo Takahashi, and Masayuki Ohzeki. Comment on "energy-time uncertainty relation for driven quantum systems" and "quantum speed limit for non-markovian dynamics", 2018.